Nonreciprocal Transport of Exciton Polaritons in a Non-Hermitian Chain

S. Mandal[,1,*] R. Banerjee[,1] Elena A. Ostrovskaya[,2] and T. C. H. Liew[1,†]

[1]*Division of Physics and Applied Physics, School of Physical and Mathematical Sciences,*
Nanyang Technological University, Singapore 637371, Singapore
[2]*ARC Centre of Excellence in Future Low-Energy Electronics Technologies and Nonlinear Physics Centre, Research School of Physics,*
The Australian National University, Canberra, ACT 2601, Australia

We consider exciton polaritons in a zigzag chain of coupled elliptical micropillars subjected to incoherent excitation. The driven-dissipative nature of the system along with the naturally present polarization splitting inside the pillars gives rise to nonreciprocal dynamics, which eventually leads to the non-Hermitian skin effect, where all the modes of the system collapse to one edge. As a result, the polaritons propagate only in one direction along the chain, independent of the excitation position, and the propagation in the opposite direction is suppressed. The system shows robustness against disorder and, using the bistable nature of polaritons to encode information, we show one-way information transfer. This paves the way for compact and robust feedback-free one-dimensional polariton transmission channels without the need for external magnetic field, which are compatible with proposals for polaritonic circuits.

Introduction.—Nonreciprocal elements, where the transfer of a signal is favored only in one direction [1], are an essential part of information processing [2]. However, designing such components in optical circuits is far from trivial due to the time-reversal invariance of Maxwell's equations. Magnetic materials can be used to achieve on-chip optical isolation but they require large external magnetic fields [3]. Other ways to achieve optical non-reciprocity, such as time-varying fields and optical non-linearity are difficult to scale down to the microscale.

Optical information processing has been a particularly prominent topic in the field of exciton polaritons, where one aims to benefit from the hybridization of an otherwise photonic system with a significant electronic nonlinearity. Polaritonic switches [4–6], transistors [6–9], amplifiers [10,11], memories [12,13], and routers [14–16] have already been realized. However, the future of this field depends on the development of mechanisms to connect elements without feedback. Here the issue of how to generate nonreciprocal behavior is as nontrivial as in other optical systems.

Significant motivation has been drawn from topological photonics, where chiral edge states have been suggested for directionally dependent connections [17,18]. Theoretically, robust polaritonic edge states can be achieved in many ways: by lifting the spin degeneracy and using spin-orbit coupling [19–26]; by realizing Hofstadter's butterfly [27]; by using nonlinear interactions [28,29]; by using staggered honeycomb lattices [30]; or by Floquet engineering [31]. The scheme in Refs. [20,21] has been realized experimentally under high external magnetic field using super-conducting coils [32]. Apart from the bulky nature of this

system, chiral edge states in this scheme appear in counter-propagating pairs, which can cause unwanted feedback. To circumvent this problem, mechanisms to switch off one of the edge states [33], to make both the edge states co-propagating [34], or to use the polariton lifetime for input or output isolation [35], have been considered. However, topological schemes remain ultimately inefficient for information transport. While plasmonic or exciton-polaritonic zigzag Su-Schrieffer-Heeger (SSH) chains [36,37] demonstrate robust topological protection of edge-localized states, they show no transport. In 2D systems, chiral topological states can propagate along the edge of the system, however, they require a large-sized bulk to separate their edges for any chance of nonreciprocity.

Here, we propose a scheme for nonreciprocal propagation of exciton polaritons in a quasi-1D geometry, which relies on inherent non-Hermiticity of the system. We make use of the recent experimental development of elliptical micropillars [38,39], where polarization splitting can be controllably engineered, and use the driven-dissipative nature of the system to demonstrate propagation in a chain of micropillars even in the presence of disorder. We derive an effective 2×2 matrix Hamiltonian describing the coupling between two different polarized modes in neighboring micropillars, which is mediated via other polarized modes. In a Hermitian system the coupling would necessarily be reciprocal. However, our effective Hamiltonian is non-Hermitian. Consequently, one of the off-diagonal elements of the matrix can vanish while the other does not, which is equivalent to a nonreciprocal coupling between two modes. In a chain of pillars, this eventually leads to the non-Hermitian skin effect, where the usual
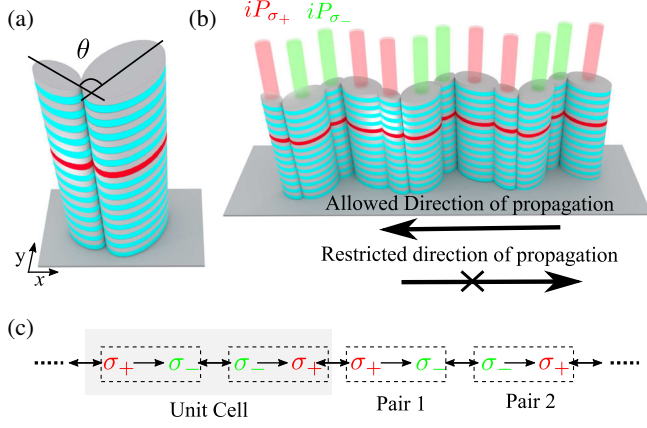
FIG. 1.   Scheme: (a) A pair of coupled elliptical micropillars of different sizes; their mutual orientation introduces the polarization splitting angle θ. (b) Micropillar pairs are arranged in a 1D zigzag chain, where each micropillar is subjected to an incoherent excitation. (c) Effective coupling mechanism between the micropillars in the lattice. Each pair of micropillars indicated by the dashed boxes has nonreciprocal coupling. The unit cell of the 1D lattice is shown by the gray box.

bulk-boundary condition breaks down and all the modes of the system become localized at one edge of the chain [40–43]. One of the key advantages of the system is that, robust propagation of polaritons through a one-dimensional chain of micropillars is obtained without the need for an external magnetic field. This compact mechanism of nonreciprocal coupling is particularly promising for future polaritonic devices. We also demonstrate the transport of binary information between localized sites where nonlinearity enables a bistable behavior.

The model.—We start by considering exciton-polariton states in a pair of coupled elliptical micropillars [Fig. 1(a)] described by the following set of driven dissipative Schrödinger equations in the tight-binding limit:

$$i\hbar\frac{\partial \psi_{\sigma_+}^l}{\partial t} = (\varepsilon + d\varepsilon/2)\psi_{\sigma_+}^l + J\psi_{\sigma_+}^r + \Delta_T e^{+2i\theta_l}\psi_{\sigma_-}^l, \quad (1)$$

$$i\hbar\frac{\partial \psi_{\sigma_-}^l}{\partial t} = (\varepsilon + d\varepsilon/2 - i\Gamma)\psi_{\sigma_-}^l + J\psi_{\sigma_-}^r + \Delta_T e^{-2i\theta_l}\psi_{\sigma_+}^l, \quad (2)$$

$$i\hbar\frac{\partial \psi_{\sigma_+}^r}{\partial t} = (\varepsilon - d\varepsilon/2 - i\Gamma)\psi_{\sigma_+}^r + J\psi_{\sigma_+}^l + \Delta_T e^{+2i\theta_r}\psi_{\sigma_-}^r, \quad (3)$$

$$i\hbar\frac{\partial \psi_{\sigma_-}^r}{\partial t} = (\varepsilon - d\varepsilon/2)\psi_{\sigma_-}^r + J\psi_{\sigma_-}^l + \Delta_T e^{-2i\theta_r}\psi_{\sigma_+}^r. \quad (4)$$

Here exciton-polariton modes in each pillar are described by a wave function having two circular polarization components, $\psi_{\sigma_\pm}$, where l and r represent the left and right pillars, respectively. We allow the modes in the left and right pillars to have different energies, where ε is their average energy and $d\varepsilon$ is their energy difference. Γ is the

dissipation due to the finite lifetime of polaritons, which is compensated [10] using an incoherent excitation for modes $\psi_{\sigma_+}^l$ and $\psi_{\sigma_-}^r$. Each pillar is coupled to its neighbor by the Josephson coupling term J. Δ_T is the polarization splitting inside each pillar which is naturally present in elliptical micropillars [39] and θ represents the angle of polarization splitting equivalent to the micropillar orientation [44]. It is helpful to shift to a rotating frame by redefining the wave functions $\psi \to \psi \exp(-i\varepsilon t/\hbar)$ such that the effective onsite energies become $\pm d\varepsilon/2$. Because of the presence of Γ, the dynamics of $\psi_{\sigma_-}^l$ and $\psi_{\sigma_+}^r$ is much faster compared to that of $\psi_{\sigma_+}^l$ and $\psi_{\sigma_-}^r$. As a result, on the timescale of $\psi_{\sigma_+}^l$ and $\psi_{\sigma_-}^r$, $\psi_{\sigma_-}^l$ and $\psi_{\sigma_+}^r$ can be approximated as stationary states

$$\psi_{\sigma_-}^l = -\frac{J\psi_{\sigma_-}^r + \Delta_T e^{-2i\theta_l}\psi_{\sigma_+}^l}{(d\varepsilon/2 - i\Gamma)}, \quad (5)$$

$$\psi_{\sigma_+}^r = -\frac{J\psi_{\sigma_+}^l + \Delta_T e^{+2i\theta_r}\psi_{\sigma_-}^r}{(-d\varepsilon/2 - i\Gamma)}. \quad (6)$$

Substituting into Eqs. (1) and (4), the dynamics of the *slow* components of the system is given by

$$i\hbar\frac{\partial}{\partial t}\begin{pmatrix} \psi_{\sigma_+}^l \\ \psi_{\sigma_-}^r \end{pmatrix} = \begin{pmatrix} H_{ll} & H_{lr} \\ H_{rl} & H_{rr} \end{pmatrix}\begin{pmatrix} \psi_{\sigma_+}^l \\ \psi_{\sigma_-}^r \end{pmatrix}, \quad (7)$$

where the effective Hamiltonian has the elements

$$H_{ll} = d\varepsilon/2 - \frac{J^2}{(-d\varepsilon/2 - i\Gamma)} - \frac{\Delta_T^2}{(d\varepsilon/2 - i\Gamma)}, \quad (8)$$

$$H_{rr} = -d\varepsilon/2 - \frac{J^2}{(d\varepsilon/2 - i\Gamma)} - \frac{\Delta_T^2}{(-d\varepsilon/2 - i\Gamma)}, \quad (9)$$

$$H_{lr} = -J\Delta_T\left[\frac{e^{2i\theta_l}}{(d\varepsilon/2 - i\Gamma)} + \frac{e^{2i\theta_r}}{(-d\varepsilon/2 - i\Gamma)}\right], \quad (10)$$

$$H_{rl} = -J\Delta_T\left[\frac{e^{-2i\theta_l}}{(d\varepsilon/2 - i\Gamma)} + \frac{e^{-2i\theta_r}}{(-d\varepsilon/2 - i\Gamma)}\right]. \quad (11)$$

Since this Hamiltonian is non-Hermitian ($H_{lr} \neq H_{rl}^*$), we can set $H_{rl} = 0$ while keeping $H_{lr} \neq 0$. Indeed, such a condition can be obtained by setting [44]

$$d\varepsilon \neq 0, \quad \text{and} \quad (\theta_r - \theta_l) = \arctan(-2\Gamma/d\varepsilon). \quad (12)$$

Note that according to Eqs. (10) and (11) it is essential that $\theta_l \neq \theta_r$, which corresponds to neighboring micropillars having different orientations, so that $H_{lr} \neq H_{rl}e^{4i\theta_l}$. The condition (12) leads to nonreciprocal coupling between the micropillars. For the above-mentioned excitation scheme, σ_+ polaritons hop from the left micropillar to the right one. It is also possible to do the same for the σ_- polaritons by
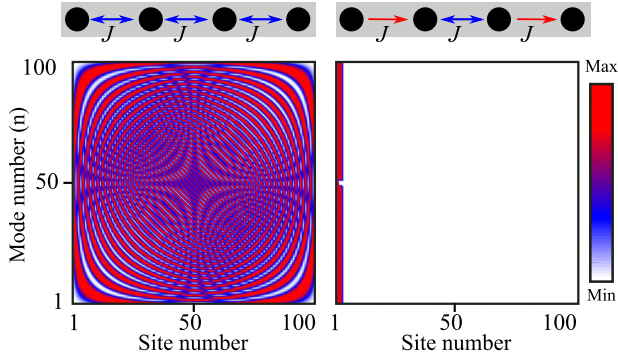
FIG. 2. Spatial profiles of different modes as a function of site number for a trivial chain of 100 micropillars (left panel) and nonreciprocal chain of 100 micropillars (right panel) in the tight binding limit. Here the blue arrows correspond to bidirectional coupling and the red arrows correspond to nonreciprocal coupling. Because of the non-Hermitian skin effect all the modes for the nonreciprocal chain collapse to the left edge. The most localized modes for $n = 50$ and 51 correspond to the zero energy modes, similar to those in Ref. [56], but located at one edge. Parameter: $J = 0.5$ meV.

interchanging the components subject to incoherent excitation [44].

The pairs of micropillars with nonreciprocal coupling can be combined into a chain [see Fig. 1(b)]. Since the nonreciprocal transmission is also flipping the spin polarization, we use one pair to transport σ_+ polarization rightward to a σ_- state, which is then coupled bidirectionally to another pair that transports the σ_- state to a σ_+ state. This gives a unit cell of four micropillars [see Fig. 1(c)]. Even though the connection between the pairs is bidirectional, the nonreciprocity within each pair ensures nonreciprocity of the whole chain. In Fig. 2 the mode profiles of a trivial chain and the nonreciprocal chain are shown. For the trivial chain, the modes are distributed over all sites while for the case of the nonreciprocal chain all the modes are located at one edge. This is known as the non-Hermitian skin effect [53–55], which occurs in non-Hermitian systems with nonreciprocity and cannot be reproduced in Hermitian systems. To obtain the non-Hermitian skin effect, it is not necessary to fully switch off one of the nondiagonal terms; a small anisotropy between them is sufficient for collapsing the modes to one edge (see Supplemental Material [44], movie 1).

Band structure and pulse propagation.—To illustrate that our results do not depend on the tight-binding approximation, we now move to a continuous model in space using the driven-dissipative Gross-Pitaevskii equation,

$$i\hbar\frac{\partial\psi_{\sigma_\pm}}{\partial t} = \left[-\frac{\hbar^2\nabla^2}{2m} + V(x,y) + i\hbar[p_{\sigma_\pm}(x,y) - \gamma(x,y)]\right.$$
$$\left. + \hbar g p_{\sigma_\pm}(x,y) + I_{\sigma_\pm}^{NL}\right]\psi_{\sigma_\pm} + V_T(x,y,\pm\theta)\psi_{\sigma_\mp}. \quad (13)$$
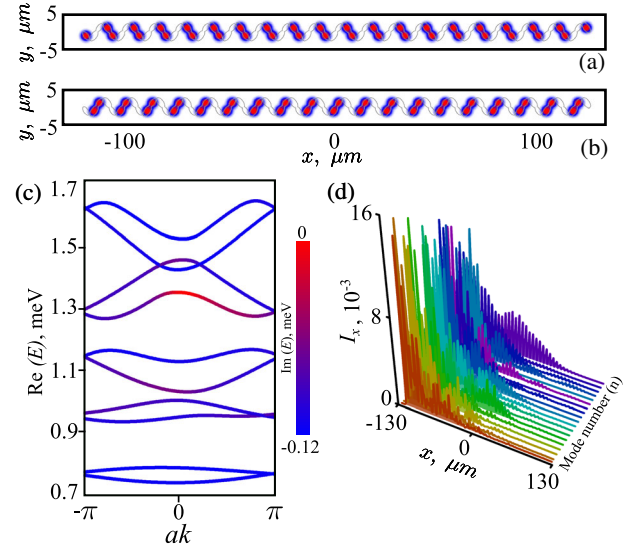

FIG. 3. (a)–(b) The spatial profile of the incoherent pumps P_{σ_+} and P_{σ_-}, respectively, composed of Gaussians of width 2.1 μm positioned at the center of the relevant micropillars. Such an arrangement is within the reach of experimental technology [58]. (c) Band structure of an infinite chain under incoherent excitation. The states shown in red correspond to the *slow* modes and decay slower than all other states shown in blue. (d) Spatial profile, $I_x = \sum_{\sigma_\pm}\int|\psi_\sigma(x,y)|^2 dy$, corresponding to the *slow* modes for the case of a finite chain. Here different colors denote different modes.

Here m is the effective polariton mass, $V(x, y)$ is the effective potential representing a zigzag chain of elliptical micropillars [see Fig. 1(b)], $p_{\sigma_\pm}$ and γ characterize the rate of injection of polaritons by the incoherent pump and the rate of polariton decay, respectively. γ outside the micropillars is two times larger than the inside. The term with the dimensionless g factor is introduced to take into account the potential created by the excitonic reservoir, which has the same profile as the incoherent excitation. $I_{\sigma_\pm}^{NL} = (\alpha_1 - i\alpha_{NL})|\psi_{\sigma_\pm}|^2 + \alpha_2|\psi_{\sigma_\mp}|^2$ is the nonlinear contribution, which includes interactions between polaritons with the same spin (with strength α_1), opposite spin (with strength α_2), and gain saturation caused by the depletion of the excitonic reservoir (with strength α_{NL}) [57]. $2V_T$ represents the polarization splitting inside the micropillars, which is modeled with the same spatial profile as V with an extra factor of $\exp(\pm 2i\theta)$ to take into account the orientation of each pillar [44]. In writing Eq. (13), we have assumed that the dynamics of the reservoir is fast and therefore its effect can be modeled by the effective gain, effective potential, and the gain saturation (α_{NL}) terms. Our results are independent of this assumption [44] and can also be reproduced with an explicit account of reservoir dynamics [52].

The incoherent pumps are arranged so that the *slow* component of the polariton mode in each micropillar has almost zero decay. The spatial profile of the incoherent pump is shown in Figs. 3(a)–3(b). Now, we have all the

ingredients to calculate the band structure of the linear system ($I_{\sigma_\pm}^{NL} = 0$) under the periodic boundary condition, which is shown in Fig. 3(c). Since there are four sites in one unit cell, the real part of the low energy band structure of the system is composed of four bands. It should be noted that this is an exact band structure of the system without the approximations used in Eqs. (5)–(6) and the states having lower decay correspond to the *slow* modes in the approximated Hamiltonian in Eq. (7). Each state in the real part of the band structure is color coded according to the imaginary part with red corresponding to the lowest decay (*slow* modes), and blue corresponding to the larger decay. The nonreciprocal nature of the system can be attributed to the fact that, the states shown in red [see the lower branch of the fourth band in Fig. 3(c)] will accumulate the polaritons relaxing from higher energy. These states have a negative group velocity, $v_g = (\partial E/\partial k)/\hbar$; whereas more lossy states have positive group velocity. Overall, we can expect to have polariton propagation at a speed v_g along only one direction in the micropillar chain. The spatial profiles of highly occupied modes plotted in Fig. 3(d) are in agreement with the modes obtained in the tight-binding limit shown in Fig. 2. Although the bulk is translationally symmetric, the localization of the modes at the left edge of the chain indicates the breakdown of the usual bulk-boundary correspondence in Hermitian systems [54].

The above band structure calculation is performed by using typical experimental parameters [59]. For the angle between the two micropillars inside one micropillar pair around 110°, the periodicity of the lattice along the x direction becomes $a = 12.9$ μm, which corresponds to $v_g = -0.7$ μm/ps. The negative value of v_g means that the polaritons propagate from right to left along the micropillar chain.

To demonstrate the nonreciprocal polariton propagation, we apply a Gaussian shaped incoherent excitation pulse in the middle of the chain. The dynamics of the polaritons can be seen in Fig. 4. Unlike a trivial chain of micropillars, where the polaritons propagate in both directions from the excitation spot [44], in this case they propagate only in one direction. As explained above, this is due to the states with lower losses acquiring a larger polariton population compared to the decaying states. Remarkably, all the polaritons in the system will be localized at the left edge of the chain, regardless of the position of the excitation spot. This is quite similar to the recently realized topological funneling of light [55]. From the intensity profile it is clear that only the *slow* components of the on-site modes get excited, and they are mostly localized in the micropillars with smaller dimension, which can be attributed to the dominant contribution of the smaller pillars to fourth band in the band structure [see Fig. 3(c)] (see the Bloch states in Ref. [44]).

Demonstration of feedback suppression.—Because of their strong nonlinearity, polaritons show bistable behavior that makes them suitable for several applications, such as
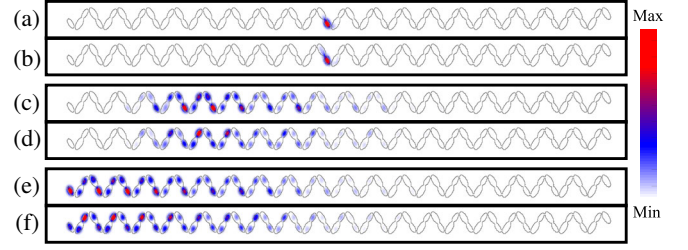

FIG. 4. (a),(c),(e) Density of the σ_+ polaritons under an incoherently pulsed excitation for 10, 90, and 180 ps, respectively. The same for the σ_- polaritons are shown in (b),(d),(f). The nonreciprocal nature of the system is clear from the fact that the polaritons propagate only in one direction while the propagation in the opposite direction is suppressed. The width of the incoherent pulse is taken as 2.1 μm and the peak power of the gain rate is taken as 14.2γ.

solving NP-hard problems [60], realizing bistable topological insulators [61,62], universal logic gates [63], and enhancement of dark soliton stability [64]. In this section we introduce additional resonant pumps placed at the two ends of the chain such that the end pillars, with the on-site wave functions $\psi_{\sigma_+}^L$ and $\psi_{\sigma_+}^R$, are initially in their lower bistable states. The bistability curves of the end pillars, plotted in Figs. 5(a)–5(b), are obtained by slowly varying the pump, F. Next, an incoherent pulse is introduced at the left end of the chain, which switches $\psi_{\sigma_+}^L$ from its lower bistable state to the upper one. Because of the nonreciprocal
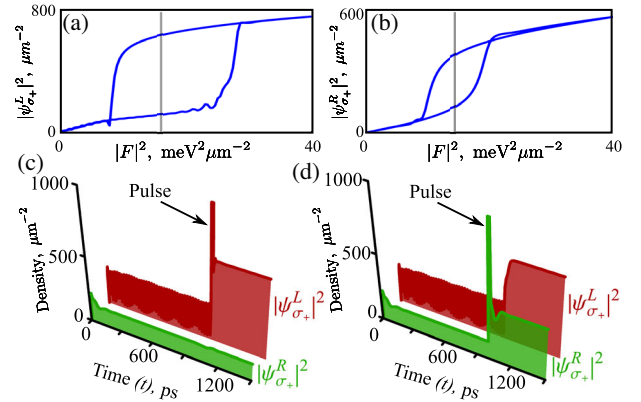

FIG. 5. (a)–(b) Bistability curves of the pillars at the left and right end of the chain, respectively. The energy of the resonant pump F is fixed at 1.38 meV. The gray line in the bistability curves represents the pump values ($F = 4.1$ meV μm^{-1} and 3.9 meV μm^{-1}, respectively, for left and right end pillars) used to demonstrate the switching. (c)–(d) Time dynamics of the end pillars when the incoherent pulse is positioned at the left and right end, respectively. Pulse positioned at the right end induces switching at both ends, whereas the pulse positioned at the left end does not switch the pillar at the right end. The spatial profile of the resonant pump and incoherent pulse are the same as the one in Fig 4. The peak value of the pulse is taken as $35p_0$. To visualize the switching effect the maximum density is cut at 10^3 μm^{-2}.

nature of the system, polaritons cannot propagate from left to right and therefore no switching is observed for $\psi_{\sigma_+}^R$ [see Fig. 5(c)]. Then, we introduce the same incoherent pulse at the right end of the chain. As expected, $\psi_{\sigma_+}^R$ switches instantly, but more importantly $\psi_{\sigma_+}^L$ also switches after some time [see Fig. 5(d)]. This can be thought of as feedback suppressed information processing, where the information is encoded in the bistability and transmitted in one direction only (from right to left). The nonlinear coefficients used for the calculations are $\alpha_1 = 1 \ \mu\text{eV} \ \mu\text{m}^2$ [65], $\alpha_2 = -0.05\alpha_1$ [66–68], and $\alpha_{NL} = 0.3\alpha_1$ [69]. Although we have modeled the scheme with resonant excitation, we expect that the nonreciprocal transport mechanism would also be compatible with bistability under nonresonant excitation [70–72].

Discussion and conclusion.—We have presented a scheme for nonreciprocal exciton-polariton transport in a quasi-1D chain of elliptical micropillars without an external magnetic field. Because of the nonreciprocal coupling within micropillar pairs, all the highly populated polariton states are localized at one edge of the chain. This makes the polaritons propagate in one direction along the chain regardless of the excitation position. This nonreciprocity also protects against backscattering (see Ref. [44] for the discussion on the robustness against disorder) and allows one-way information transfer. While our theory is restricted to the semiclassical regime, it would be interesting to extend it to the quantum optical regime, where nonreciprocal blockade effects are anticipated [73]. Because of its compactness, such a chain can be extremely useful in connecting different components of future polaritonic circuits such as the polariton neural networks [74,75].

*Corresponding author.
 subhaska001@e.ntu.edu.sg
†Corresponding author.
 tchliew@gmail.com

[1] C. Caloz, A. Alu, S. Tretyakov, D. Sounas, K. Achouri, and Z. L. D. Leger, Electromagnetic Nonreciprocity, Phys. Rev. Applied 10, 047001 (2018).

[2] R. W. Keyes, What makes a good computer device?, Science 230, 138 (1985).

[3] L. Bi, J. Hu, P. Jiang, D. H. Kim, G. F. Dionne, L. C. Kimerling, and C. A. Ross, On-chip optical isolation in monolithically integrated non-reciprocal optical resonators, Nat. Photonics 5, 758 (2011).

[4] G. Grosso, S. Trebaol, M. Wouters, F. Morier-Genoud, M. T. Portella-Oberli, and B. Deveaud, Nonlinear relaxation and selective polychromatic lasing of confined polaritons, Phys. Rev. B 90, 045307 (2014).

[5] A. Dreismann, H. Ohadi, Y. D. V. Redondo, R. Balili, Y. G. Rubo, S. I. Tsintzos, G. Deligeorgis, Z. Hatzopoulos, P. G. Savvidis, and J. J. Baumberg, A sub-femtojoule electrical spin-switch based on optically trapped polariton condensates, Nat. Mater. 15, 1074 (2016).

[6] P. Lewandowski, S. M. H. Luk, C. K. P. Chan, P. T. Leung, N. H. Kwong, R. Binder, and S. Schumacher, Directional optical switching and transistor functionality using optical parametric oscillation in a spinor polariton fluid, Opt. Express 25, 31056 (2017).

[7] T. Gao, P. S. Eldridge, T. C. H. Liew, S. I. Tsintzos, G. Stavrinidis, G. Deligeorgis, Z. Hatzopoulos, and P. G. Savvidis, Polariton condensate transistor switch, Phys. Rev. B 85, 235102 (2012).

[8] D. Ballarini, M. De Giorgi, E. Cancellieri, R. Houdre, E. Giacobino, R. Cingolani, A. Bramati, G. Gigli, and D. Sanvitto, All-optical polariton transistor, Nat. Commun. 4, 1778 (2013).

[9] A. V. Zasedatelev, A. V. Baranikov, D. Urbonas, F. Scafir- imuto, Ul. Scherf, T. Stoferle, R. F. Mahrt, and P. G. Lagoudakis, A room-temperature organic polariton transistor, Nat. Photonics 13, 378 (2019).

[10] E. Wertz, A. Amo, D. D. Solnyshkov, L. Ferrier, T. C. H. Liew, D. Sanvitto, P. Senellart, I. Sagnes, A. Lemaitre, A. V. Kavokin, G. Malpuech, and J. Bloch, Propagation and Amplification Dynamics of 1D Polariton Condensates, Phys. Rev. Lett. 109, 216404 (2012).

[11] D. Niemietz, J. Schmutzler, P. Lewandowski, K. Winkler, M. Aßmann, S. Schumacher, S. Brodbeck, M. Kamp, C. Schneider, S. Höfling, and M. Bayer, Experimental realization of a polariton beam amplifier, Phys. Rev. B 93, 235301 (2016).

[12] X. Ma and S. Schumacher, Vortex-vortex control in exciton-polariton condensates, Phys. Rev. B 95, 235301 (2017).

[13] X. Ma, B. Berger, M. Aßmann, R. Driben, T. Meier, C. Schneider, S. Höfling, and S. Schumacher, Realization of all-optical vortex switching in exciton-polariton condensates, Nat. Commun. 11, 897 (2020).

[14] H. Flayac and I. G. Savenko, An exciton-polariton mediated all-optical router, Appl. Phys. Lett. 103, 201105 (2013).

[15] F. Marsault, H. S. Nguyen, D. Tanese, A. Lemaitre, E. Galopin, I. Sagnes, A. Amo, and J. Bloch, Realization of an all optical exciton-polariton router, Appl. Phys. Lett. 107, 201115 (2015).

[16] J. Schmutzler, P. Lewandowski, M. Aßmann, D. Niemietz, S. Schumacher, M. Kamp, C. Schneider, S. Höfling, and M. Bayer, All-optical flow control of a polariton condensate using nonresonant excitation, Phys. Rev. B 91, 195308 (2015).

[17] L. Lu, J. D. Joannopoulos, and M. Soljacic, Topological photonics, Nat. Photonics 8, 821 (2014).

[18] T. Ozawa, H. M. Price, A. Amo, N. Goldman, M. Hafezi, L. Lu, M. C. Rechtsman, D. Schuster, J. Simon, O. Zilberberg, and I. Carusotto, Topological photonics, Rev. Mod. Phys. 91, 015006 (2019).

[19] T. Karzig, C. E. Bardyn, N. H. Lindner, and G. Refael, Topological Polaritons, Phys. Rev. X 5, 031001 (2015).

[20] C. E. Bardyn, T. Karzig, G. Refael, and T. C. H. Liew, Topological polaritons and excitons in garden-variety systems, Phys. Rev. B 91, 161413(R) (2015).

[21] A. V. Nalitov, D. D. Solnyshkov, and G. Malpuech, Polariton Z Topological Insulator, Phys. Rev. Lett. 114, 116401 (2015).

[22] D. R. Gulevich, D. Yudin, D. V. Skryabin, I. V. Iorsh, and I. A. Shelykh, Exploring nonlinear topological states of matter with exciton-polaritons: Edge solitons in kagome lattice, Sci. Rep. **7**, 1780 (2017).

[23] Y. V. Kartashov and D. V. Skryabin, Bistable Topological Insulator with Exciton-Polaritons, Phys. Rev. Lett. **119**, 253904 (2017).

[24] C. Li, F. Ye, X. Chen, Y. V. Kartashov, A. Ferrando, L. Torner, and D. V. Skryabin, Lieb polariton topological insulators, Phys. Rev. B **97**, 081103(R) (2018).

[25] M. Sun, D. Ko, D. Leykam, V. M. Kovalev, and I. G. Savenko, Exciton-Polariton Topological Insulator with an Array of Magnetic Dots, Phys. Rev. Applied **12**, 064028 (2019).

[26] H. Sigurdsson, Y. S. Krivosenko, I. V. Iorsh, I. A. Shelykh, and A. V. Nalitov, Spontaneous topological transitions in a honeycomb lattice of exciton-polariton condensates due to spin bifurcations, Phys. Rev. B **100**, 235444 (2019).

[27] R. Banerjee, T. C. H. Liew, and O. Kyriienko, Realization of Hofstadter's butterfly and a one-way edge mode in a polaritonic system, Phys. Rev. B **98**, 075412 (2018).

[28] C. E. Bardyn, T. Karzig, G. Refael, and T. C. H. Liew, Chiral Bogoliubov excitations in nonlinear bosonic systems, Phys. Rev. B **93**, 020502(R) (2016).

[29] H. Sigurdsson, G. Li, and T. C. H. Liew, Spontaneous and superfluid chiral edge states in exciton-polariton condensates, Phys. Rev. B **96**, 115453 (2017).

[30] O. Bleu, G. Malpuech, and D. D. Solnyshkov, Robust quantum valley Hall effect for vortices in an interacting bosonic quantum fluid, Nat. Commun. **9**, 3991 (2018).

[31] R. Ge, W. Broer, and T. C. H. Liew, Floquet topological polaritons in semiconductor microcavities, Phys. Rev. B **97**, 195305 (2018).

[32] S. Klembt, T. H. Harder, O. A. Egorov, K. Winkler, R. Ge, M. A. Bandres, M. Emmerling, L. Worschech, T. C. H. Liew, M. Segev, C. Schneider, and S. Höfling, Exciton-polariton topological insulator, Nature (London) **562**, 552 (2018).

[33] S. Mandal, R. Banerjee, and T. C. H. Liew, One-Way Reflection-Free Exciton-Polariton Spin-Filtering Channel, Phys. Rev. Applied **12**, 054058 (2019).

[34] S. Mandal, R. Ge, and T. C. H. Liew, Antichiral edge states in an exciton polariton strip, Phys. Rev. B **99**, 115423 (2019).

[35] D. D. Solnyshkov, O. Bleu, and G. Malpuech, Topological optical isolator based on polariton graphene, Appl. Phys. Lett. **112**, 031106 (2018).

[36] P. St Jean, V. Goblot, E. Galopin, A. Lematre, T. Ozawa, L. Le Gratiet, I. Sagnes, J. Bloch, and A. Amo, Lasing in topological edge states of a one-dimensional lattice, Nat. Photonics **11**, 651 (2017).

[37] A. Poddubny, A. Miroshnichenko, A. Slobozhanyuk, and Y. Kivshar, Topological majorana states in zigzag chains of plasmonic nanoparticles, ACS Photonics **1**, 101 (2014).

[38] M. Klaas, O. A. Egorov, T. C. H. Liew, A. Nalitov, V. Markovic, H. Suchomel, T. H. Harder, S. Betzold, E. A. Ostrovskaya, A. Kavokin, S. Klembt, S. Höfling, and C. Schneider, Nonresonant spin selection methods and polarization control in exciton-polariton condensates, Phys. Rev. B **99**, 115303 (2019).

[39] S. Gerhardt, M. Deppisch, S. Betzold, T. H. Harder, T. C. H. Liew, A. Predojević, S. Höfling, and C. Schneider, Polarization-dependent light-matter coupling and highly indistinguishable resonant fluorescence photons from quantum dot-micropillar cavities with elliptical cross section, Phys. Rev. B **100**, 115305 (2019).

[40] C. H. Lee and R. Thomale, Anatomy of skin modes and topology in non-Hermitian systems, Phys. Rev. B **99**, 201103(R) (2019).

[41] S. Yao and Z. Wang, Edge States and Topological Invariants of Non-Hermitian Systems, Phys. Rev. Lett. **121**, 086803 (2018).

[42] A. Ghatak, M. Brandenbourger, J. v. Wezel, and C. Coulais, Observation of non-Hermitian topology and its bulk-edge correspondence, arXiv:1907.11619.

[43] L. Xiao, T. Deng, K. Wang, G. Zhu, Z. Wang, W. Yi, and P. Xue, Non-Hermitian bulk-boundary correspondence in quantum dynamics, Nat. Phys. **16**, 761 (2020).

[44] See Supplemental Material at http://link.aps.org/supplemental/10.1103/PhysRevLett.125.123902 for the realization of the polarization splitting angle, for the derivation of the conditions for nonreciprocity, for the propagation of polaritons in an ordinary polariton chain, for the spatial profile of the Bloch states, for the dependence on the nonlinear coefficients, for calculations including excitonic reservoir, and for the discussion about robustness against disorders, efficiency of the system, and material realization, which includes Refs. [38,45–52].

[45] T. Heuser, J. Große, A. Kaganskiy, D. Brunner, and S. Reitzenstein, Fabrication of dense diameter-tuned quantum dot micropillar arrays for applications in photonic information processing, APL Photonics **3**, 116103 (2018).

[46] F. Baboux, L. Ge, T. Jacqmin, M. Biondi, E. Galopin, A. Lemaître, L. Le Gratiet, I. Sagnes, S. Schmidt, H. E. Tureci, A. Amo, and J. Bloch, Bosonic Condensation and Disorder Induced Localization in a Flat Band, Phys. Rev. Lett. **116**, 066402 (2016).

[47] E. Kammann, T. C. H. Liew, H. Ohadi, P. Cilibrizzi, P. Tsotsis, Z. Hatzopoulos, P. G. Savvidis, A. V. Kavokin, and P. G. Lagoudakis, Nonlinear Optical Spin Hall Effect and Long- Range Spin Transport in Polariton Lasers, Phys. Rev. Lett. **109**, 036404 (2012).

[48] X. Ma, O. A. Egorov, and S. Schumacher, Creation and Manipulation of Stable Dark Solitons and Vortices in Microcavity Polariton Condensates, Phys. Rev. Lett. **118**, 157401 (2017).

[49] D. Bajoni, P. Senellart, E. Wertz, I. Sagnes, A. Miard, A. Lemaître, and J. Bloch, Polariton Laser Using Single Micropillar GaAs—GaAlAs Semiconductor Cavities, Phys. Rev. Lett. **100**, 047401 (2008).

[50] R. Su, S. Ghosh, J. Wang, S. Liu, C. Diederichs, T. C. H. Liew, and Q. Xiong, Observation of exciton polariton condensation in a perovskite lattice at room temperature, Nat. Phys. **16**, 301 (2020).

[51] M. Dusel, S. Betzold, O. A. Egorov, S. Klembt, J. Ohmer, U. Fischer, S. Hofling, and C. Schneider, Room temperature organic excitonpolariton condensate in a lattice, Nat. Commun. **11**, 2863 (2020).

[52] M. Wouters and I. Carusotto, Excitations in a Nonequilibrium Bose-Einstein Condensate of Exciton Polaritons, Phys. Rev. Lett. **99**, 140402 (2007).

[53] N. Okuma, K. Kawabata, K. Shiozaki, and M. Sato, Topological Origin of Non-Hermitian Skin Effects, Phys. Rev. Lett. **124**, 086801 (2020).

[54] T. Helbig, T. Hofmann, S. Imhof, M. Abdelghany, T. Kiessling, L. W. Molenkamp, C. H. Lee, A. Szameit, M. Greiter, and R. Thomale, Generalized bulk–boundary correspondence in non-Hermitian topolectrical circuits, Nat. Phys. **16**,747 (2020).

[55] S. Weidemann, M. Kremer, T. Helbig, T. Hofmann, A. Stegmaier, M. Greiter, R. Thomale, and A. Szameit, Topological funneling of light, Science https://doi.org/10.1126/science.aaz8727 (2020).

[56] P. Comaron, V. Shahnazaryan, W. Brzezicki, T. Hyart, and M. Matuszewski, Non-Hermitian topological end-mode lasing in polariton systems, Phys. Rev. Research **2**, 022051(R) (2020).

[57] M. O. Borgh, J. Keeling, and N. G. Berloff, Spatial pattern formation and polarization dynamics of a nonequilibrium spinor polariton condensate, Phys. Rev. B **81**, 235302 (2010).

[58] J. D. Töpfer, H. Sigurdsson, L. Pickup, and P. G. Lagoudakis, Time-delay polaritonics, Commun. Phys. **3**, 2 (2020).

[59] We use the elliptical micropillars with semimajor axes of 3 and 2.4 μm; semiminor axes of 1.5 and 1.2 μm, respectively; and 2 meV potential depth. The polarization splitting inside the micropillars is kept at 0.4 meV, which can be adjusted by changing the ellipticity of the micropillars [39]. The mass of the polariton is taken as $m = 3 \times 10^{-5}m_e$, where m_e is the free electron mass. The decay parameter γ inside the micropillar is 0.24 ps^{-1}, which corresponds to a polariton lifetime of 2 ps. The peak power of the gain rate of the incoherent pump is taken as, $p_0 = 2.83\gamma$, and the blueshift due to the excitonic reservoir is taken around 0.16 meV.

[60] O. Kyriienko, H. Sigurdsson, and T. C. H. Liew, Probabilistic solving of NP-hard problems with bistable nonlinear optical networks, Phys. Rev. B **99**, 195301 (2019).

[61] Y. V. Kartashov and D. V. Skryabin, Bistable Topological Insulator with Exciton-Polaritons, Phys. Rev. Lett. **119**, 253904 (2017).

[62] R. Banerjee, S. Mandal, and T. C. H. Liew, Coupling between Exciton-Polariton Corner Modes through Edge States, Phys. Rev. Lett. **124**, 063901 (2020).

[63] T. Espinosa-Ortega and T. C. H. Liew, Complete architecture of integrated photonic circuits based on AND and NOT logic gates of exciton polaritons in semiconductor microcavities, Phys. Rev. B **87**, 195305 (2013).

[64] G. Lerario, S. V. Koniakhin, A. Maitre, D. Solnyshkov, A. Zilio, Q. Glorieux, G. Malpuech, E. Giacobino, S. Pigeon, and A. Bramati, Parallel dark soliton pair in a bistable 2D exciton-polariton superfluid, arXiv:2003.11408.

[65] The polariton-polariton interaction strength α_1 is given by the exciton-exciton interaction strength multiplied by the square of the excitonic fraction. The exciton-exciton interaction strength is estimated as $6E_B a_B^2$ [76], where E_B is the exciton binding energy and a_B is the Bohr radius. Considering the typical values $E_B \approx 10$ meV and $a_B \approx 10$ nm for GaAs quantum wells, and taking the Hopfield coefficient near zero exciton-photon detuning ($|X|^2 \approx 1/2$), we estimate $\alpha_1 \sim 1$ μeV μm^2. This is also in agreement with the

[66] recent measurements [77,78]. Although the exact value changes with the Hopfield coefficient, we verified (in the Supplemental Material [44]) that our results are not sensitive to the choice of α_1.

[66] K. V. Kavokin, P. Renucci, T. Amand, X. Marie, P. Senellart, J. Bloch, and B. Sermage, Linear polarisation inversion: A signature of Coulomb scattering of cavity polaritons with opposite spins, Phys. Status Solidi C **2**, 763 (2005).

[67] M. Vladimirova, S. Cronenberger, D. Scalbert, K. V. Kavokin, A. Miard, A. Lemaître, J. Bloch, D. Solnyshkov, G. Malpuech, and A. V. Kavokin, Polariton-polariton interaction constants in microcavities, Phys. Rev. B **82**, 075301 (2010).

[68] T. Lecomte, D. Taj, A. Lemaitre, J. Bloch, C. Delalande, J. Tignon, and P. Roussignol, Polariton-polariton interaction potentials determination by pump-probe degenerate scattering in a multiple microcavity, Phys. Rev. B **89**, 155308 (2014).

[69] J. Keeling and N. G. Berloff, Spontaneous Rotating Vortex Lattices in a Pumped Decaying Condensate, Phys. Rev. Lett. **100**, 250401 (2008).

[70] D. V. Karpov, I. G. Savenko, H. Flayac, and N. N. Rosanov, Dissipative soliton protocols in semiconductor microcavities at finite temperatures, Phys. Rev. B **92**, 075305 (2015).

[71] H. Ohadi, A. Dreismann, Y. G. Rubo, F. Pinsker, Y. del Valle-Inclan Redondo, S. I. Tsintzos, Z. Hatzopoulos, P. G. Savvidis, and J. J. Baumberg, Spontaneous Spin Bifurcations and Ferromagnetic Phase Transitions in a Spinor Exciton-Polariton Condensate, Phys. Rev. X **5**, 031002 (2015).

[72] C. Zhang and G. Jin, Rotation of exciton-polariton condensates with TE-TM splitting in a microcavity ring, New J. Phys. **19**, 093002 (2017).

[73] H. Z. Shen, Qiu Wang, Jiao Wang, and X. X. Yi, Nonreciprocal unconventional photon blockade in a driven dissipative cavity with parametric amplification, Phys. Rev. A **101**, 013826 (2020).

[74] A. Opala, S. Ghosh, T. C. H. Liew, and M. Matuszewski, Neuromorphic Computing in Ginzburg-Landau Polariton-Lattice Systems, Phys. Rev. Applied **11**, 064029 (2019).

[75] D. Ballarini, A. Gianfrate, R. Panico, A. Opala, S. Ghosh, L. Dominici, V. Ardizzone, M. De Giorgi, G. Lerario, G. Gigli, T. C. H. Liew, M. Matuszewski, and D. Sanvitto, Polaritonic neuromorphic computing outperforms linear classifiers, https://doi.org/10.1021/acs.nanolett.0c00435.

[76] F. Tassone and Y. Yamamoto, Exciton-exciton scattering dynamics in a semiconductor microcavity and stimulated scattering into polaritons, Phys. Rev. B **59**, 10830 (1999).

[77] E. Estrecho, T. Gao, N. Bobrovska, D. Comber-Todd, M. D. Fraser, M. Steger, K. West, L. N. Pfeiffer, J. Levinsen, M. M. Parish, T. C. H. Liew, M. Matuszewski, D. W. Snoke, A. G. Truscott, and E. A. Ostrovskaya, Direct measurement of polariton-polariton interaction strength in the Thomas-Fermi regime of exciton-polariton condensation, Phys. Rev. B **100**, 035306 (2019).

[78] M. Pieczarka, E. Estrecho, M. Boozarjmehr, O. Bleu, M. Steger, K. West, L. N. Pfeiffer, D. W. Snoke, J. Levinsen, M. M. Parish, A. G. Truscott, and E. A. Ostrovskaya, Observation of quantum depletion in a non-equilibrium excitonpolariton condensate, Nat. Commun. **11**, 429 (2020).